Carbohydrate Polymers 104 (2014) 94–100

Contents lists available at ScienceDirect

Carbohydrate Polymers

journal homepage: www.elsevier.com/locate/carbpol

The influence of the six constituent xanthan repeating units on the order–disorder transition of xanthan

Marijn M. Kool [a], Harry Gruppen [a], Graham Sworn [b], Henk A. Schols [a,*]

[a] Wageningen University, Laboratory of Food Chemistry, P.O. Box 17, 6700 AA Wageningen, The Netherlands
[b] DUPONT, Danisco France SAS, 20 rue Brunel, 75017 Paris, France

ARTICLE INFO

Article history:
Received 30 October 2013
Received in revised form
23 December 2013
Accepted 25 December 2013
Available online 18 January 2014

Keywords:
LC–MS
Degree of substitution
Transitional behavior
Acetylation pattern
Cellulases

ABSTRACT

Xanthans occurring in different levels of disordered conformation were enzymatically hydrolyzed to their six pentamer repeating units (RUs). The RUs present in the enzyme digests were analyzed using LC–MS. As only disordered xanthan segments are degraded by cellulases, the influence of the six different RUs on the transitional behavior of xanthan could be studied. The results indicate that especially xanthan segments rich in RUs that are acetylated on the outer mannose unit stabilize the xanthan conformation. Acetylation of the inner mannose did not show to have a clear stabilizing effect on the xanthan conformation. As the enzymatic release of pyruvylated RUs gradually increased with increasing levels of disordered xanthan segments, it is concluded that the distribution of these RUs is random. On the contrary, single and double acetylated RUs are distributed over specific xanthan segments as these RUs were instantly hydrolyzed.

1. Introduction

Xanthan is a polysaccharide that gives solutions with high pseudoplastic flows, when dissolved in water (Jeanes, Pittsley, & Senti, 1961). This solution property holds over a wide pH and temperature range, making xanthan very suitable as viscosifier and/or stabilizer for the food industry (Morrison, Clark, Talashek, & Yuan, 2004; Sworn, 2009). The stability of a xanthan solution is mainly addressed to the helical conformation of xanthan (Morris, 1977). The stability of this conformation depends on the temperature and salt concentration of the solvent as well as on the primary xanthan structure (Liu & Norisuye, 1988a; Matsuda, Biyajima, & Sato, 2009; Shatwell, Sutherland, Dea, & Ross-Murphy, 1990). Xanthan is a bacterial exo-polysaccharide that consists of a β-(1 → 4) linked glucose backbone, with a (3 → 1) linked α-D-mannose-(2 → 1)-β-D-glucuronic acid-(4 → 1)-β-D-mannose side chain attached to every other glucose unit (Fig. 1) (Jansson, Kenne, & Lindberg, 1975). Variations in the primary xanthan structure are mainly due to the substituents present in the side chains. On average 85% of all inner mannose units are acetylated at the *O*-6 position and 50% of all outer mannose units carry a pyruvate group (Cadmus et al., 1976; Orentas, Sloneker, & Jeanes, 1963). The presence of acetyl groups is reported to stabilize the helical conformation (Morrison et al., 2004), while pyruvate groups destabilize the helical conformation (Sandford et al., 1977; Shatwell et al., 1990). It is generally assumed that only the inner mannose unit can be acetylated and the stabilizing effect of the acetyl groups is directed to hydrogen bonds formed with the xanthan backbone (Pelletier, Viebke, Meadows, & Williams, 2001; Tako & Nakamura, 1984). However, in a recent study we showed that xanthan consists of 6 different repeating units and that depending on the production conditions, 5–20% of all xanthan side chains are acetylated on the outer mannose units (Kool, Gruppen, Sworn, & Schols, 2013). Thereby, the question arises whether the substitution of the acetyl group on either the inner or outer mannose is important for its stabilizing effect on the xanthan conformation. It was also shown that the total degree of substitution on the outer mannose is rather constant, while the pyruvate:acetate ratio on the outer mannose depends on the fermentation conditions (Kool, Gruppen, et al., 2013). It is, therefore, plausible to postulate that the adverse effect of acetyl and pyruvate groups on the stability of the xanthan conformation is due to the type of substitution at the outer mannose unit: acetate or pyruvate. This could indicate that the location of the acetyl group within the side chain indeed is important for the stability of the xanthan conformation. If so, it could be that the results obtained in previous studies, that assume that only the inner mannose unit can be acetylated, were misinterpreted and have not always led to the proper explanation. Hence, the aim of the present study is to better understand the influence of the primary xanthan structure and the acetylation pattern, on the stability of the xanthan conformation.

* Corresponding author. Tel.: +31 317 482239.
E-mail address: henk.schols@wur.nl (H.A. Schols).

0144-8617/$ – see front matter © 2014 Elsevier Ltd. All rights reserved.
http://dx.doi.org/10.1016/j.carbpol.2013.12.073

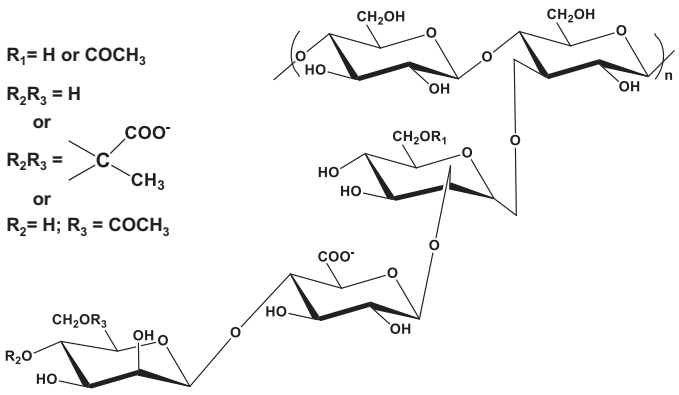

Fig. 1. The xanthan repeating structure.

2. Materials and methods

2.1. Xanthan samples

Three types of renatured xanthan, differing in acetyl and pyruvyl contents, were obtained from DuPont (Melle, France). The molecular composition of the samples and the relative abundance of the repeating units present were measured as described previously (Kool, Gruppen, et al., 2013). An overview of the xanthan compositions is given in Table 1. Based on molar compositions xanthans A and B are rather similar. Variations between these xanthans exist in their substitution patterns, where xanthan A has more acetyl groups on the outer mannose than xanthan B. Xanthan C is rich in pyruvate groups and has a relatively low level of acetylation compared to the other two xanthans. This translates into a low degree of acetylation on the outer mannose compared to xanthans A and B.

2.2. Enzymatic hydrolysis

Solutions containing 2 mg ml^{-1} xanthan A were prepared in 0, 2 and 10 mM NaCl and solutions containing 2 mg ml^{-1} xanthan B or xanthan C were prepared in 0 and 10 mM NaCl. Xanthan was hydrolyzed by incubating 1 ml of a xanthan solution with 60 μg protein from the experimental cellulase mixture C1–G1 from *Myceliophthora thermophila* C1 (Dyadic Netherlands, Wageningen, The Netherlands). The cellulase mixture was desalted prior to incubation using Micro Bio-Spin chromatography columns following the company's description (Bio-Rad Laboratories, Hercules, CA, USA).

Incubations were performed at temperatures ranging from 30 to 60 °C and continued for 48 h in order to obtain the end point of the enzymatic degradation. After hydrolysis, the digests were cooled to 6 °C.

2.3. Circular dichroism

The xanthan conformation at the enzyme incubations chosen was determined using circular dichroism. The transition profiles of the three xanthans, in 0, 2 and 10 mM NaCl solutions, were determined as described previously (Kool, Schols et al., 2013) and used to estimate the fraction of disordered xanthan (α) in the different enzyme incubations using Eq. (1) with θ_t, ellipticity at a given temperature; θ_U, ellipticity of a completely disordered structure and θ_F, ellipticity of a completely ordered structure (Greenfield, 2006).

$$a = \frac{1 - (\theta_t - \theta_U)}{\theta_F - \theta_U} \quad (1)$$

The minimum and maximum ellipticities were determined for each type of xanthan, θ_F was determined in 10 mM NaCl solutions at 15 °C and θ_U was determined in demineralized water at 85 °C. The curves obtained were normalized by the best-fit parameters in order to determine the exact fraction of disordered conformation at all enzyme incubation conditions chosen.

2.4. High performance size exclusion chromatography (HPSEC)

HPSEC was performed on an Ultimate 3000 system (Dionex, Sunnyvale, CA, USA) as described previously (Kool, Schols, et al., 2013). Apparent molecular mass distributions were estimated using pullulan molecular-mass standards (Polymer Laboratories, Palo Alto, CA, USA). Xanthan digests were centrifuged (10,000 × *g*; 10 min; 25 °C) prior to injection.

Table 1
Molar composition of different xanthan samples.

Xanthan type	Glc:Man:GlcA Molar Ratio	Acetyl content (w/w%)	Pyruvate content (w/w%)	RU-1	RU-2	RU-3	RU-4	RU-5	RU-6	Ac:Pyr-ratio on the outer mannose
Xanthan A	1:0.88:0.41	5.6	4.4	19	11	2	62	2	4	1:3.1
Xanthan B	1:0.91:0.43	5.9	4.6	14	12	1	67	2	4	1:4.7
Xanthan C	1:0.94:0.45	4.8	7.3	4	2	1	77	1	15	1:18.4

● glucose; ● mannose; ⊘ glucuronic acid; ○ acetyl groups; ● pyruvic acid ketal

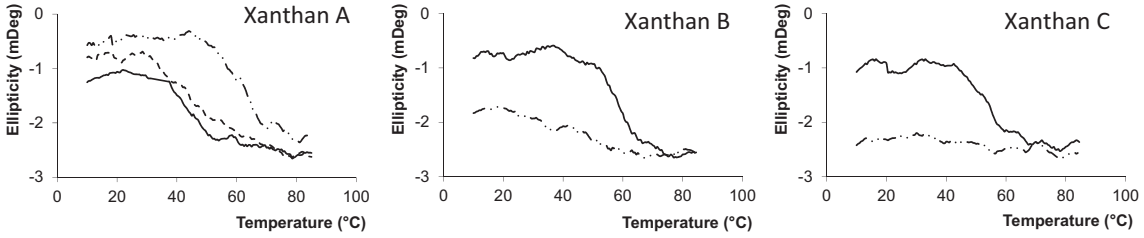

Fig. 2. Transition profiles of xanthan in: deionized water (——), 2 mM NaCl (.....) and 10 mM NaCl (– – – –).

Table 2
Enzyme incubation conditions and the corresponding fraction of xanthan present in a disordered conformation (α).

Xanthan	Salt concentration (mM NaCl)	Temperature (°C)	Fraction of disordered conformation (α)
Xanthan A	10	30	0
		40	0
		50	0.05
		60	0.38
	0	30	0.42
		40	0.52
		50	0.93
		60	1
Xanthan B	10	30	0
		40	0
		50	0.11
		60	0.55
	0	30	0.58[a]
		40	0.62
		50	0.75
		60	1
Xanthan C	10	30	0
		40	0.03
		50	0.32
		60	0.82
	0	30	0.87[a]
		40	0.91
		50	0.95[a]
		60	1

[a] HILIC-ESLD results are not further shown, as results were equal to the results of other digests of the same xanthan obtained at a similar α.

2.5. HILIC-ELSD–ESI-IT-MS^n

Digests were analyzed using UPLC-ELSD-MS^n on a HILIC BEH amide column (Waters Corporation, Milford, MA, USA), which was coupled to an ELSD and an ESI-MS^n-detector as described elsewhere (Kool, Gruppen, et al., 2013). The xanthan digests were filtered using Amicon-0.5 mL centrifugal filter devices with a 10 kDa cut off (EMD Millipore Corporation, Billerica, MA, USA) to remove any remaining high molecular weight xanthan. The filtrate was diluted 1:1 (v:v) with milliQ water followed by a 1:1 (v:v) dilution with acetonitrile before injection into the system.

The ELSD peak area was used to determine the ratio in which the different xanthan repeating units (RUs) were present in the xanthan digests (Kool, Gruppen, et al., 2013). The peak areas of the different RUs of fully degraded xanthan, obtained after incubation under conditions in which $\alpha = 1$, were used to determine the maximum ELSD-peak area for each type of RU. As the two single acetylated RU elute simultaneously, the MS-fragmentation pattern was used to distinguish and semi-quantify between the RUs which are solely acetylated at the inner or outer mannose (Kool, Gruppen, et al., 2013). To determine which part of each specific RU was released at a given xanthan conformation, the ELSD peak areas of each RU present in digests obtained at $\alpha < 1$, are expressed as % of the maximum ESLD peak area of that RU.

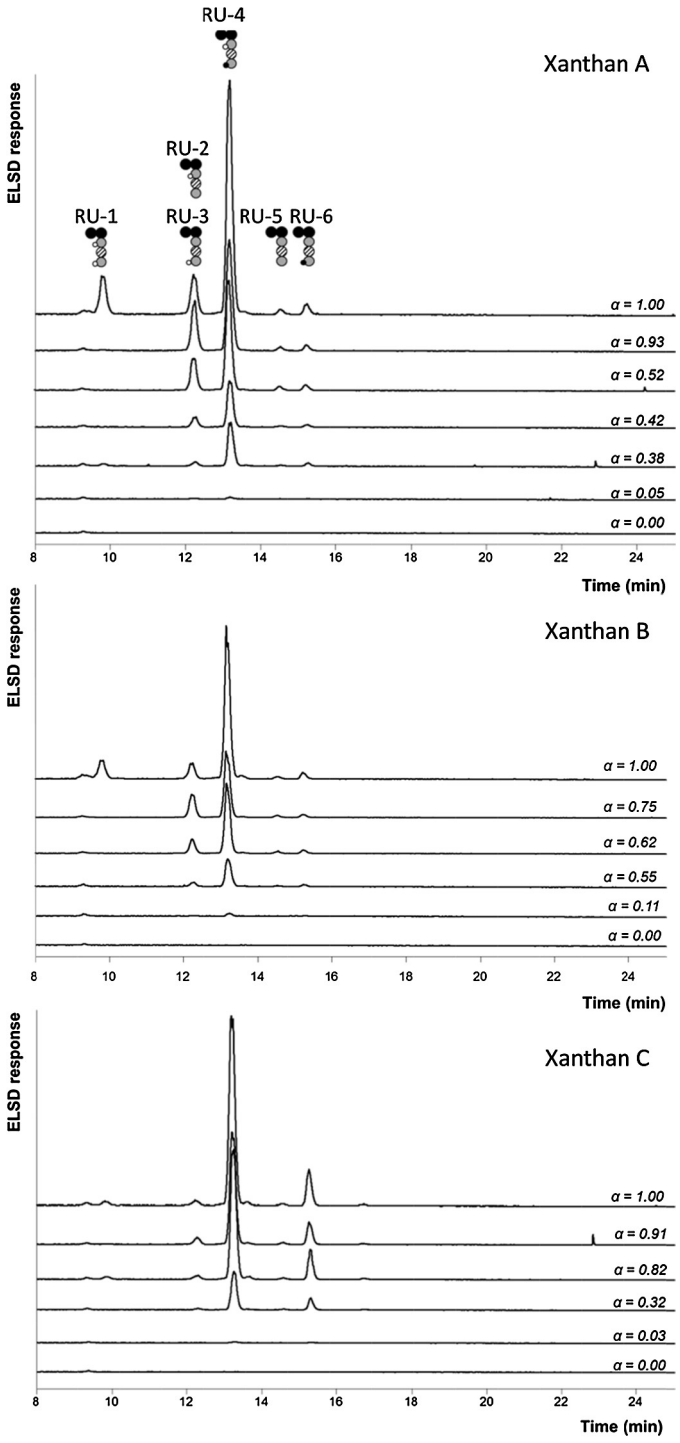

Fig. 3. HILIC-ELSD elution profiles of xanthan digests obtained after a 48 h incubation with cellulases at different fraction of disordered conformation (α). Glucose (●); mannose (◍); glucuronic acid (◪); acetyl group (○); pyruvic acid acetal (●).

3. Results and discussion

3.1. Order–disorder transitions

The transition profiles of the three xanthans, obtained through CD analysis, are shown in Fig. 2. It can be concluded that xanthan C exhibits the lowest mid-point transition temperature (T_m). This was expected, as xanthan C has the highest pyruvate content, which destabilizes the ordered conformation (Shatwell et al., 1990). Xanthans A and B have lower levels of pyruvylation and higher levels of acetylation compared to xanthan C. Thereby, they have a higher T_m compared to xanthan C. This correlation has been reported before for other xanthans (Rinaudo, 2004; Shatwell et al., 1990). Although xanthans A and B have a rather similar molecular composition (Table 1), their transitional behavior, as determined by CD, is different: xanthan B has lower transition temperatures than xanthan A, indicating a less stable ordered conformation (Rinaudo, 2004; Shatwell et al., 1990). This difference is most likely the result

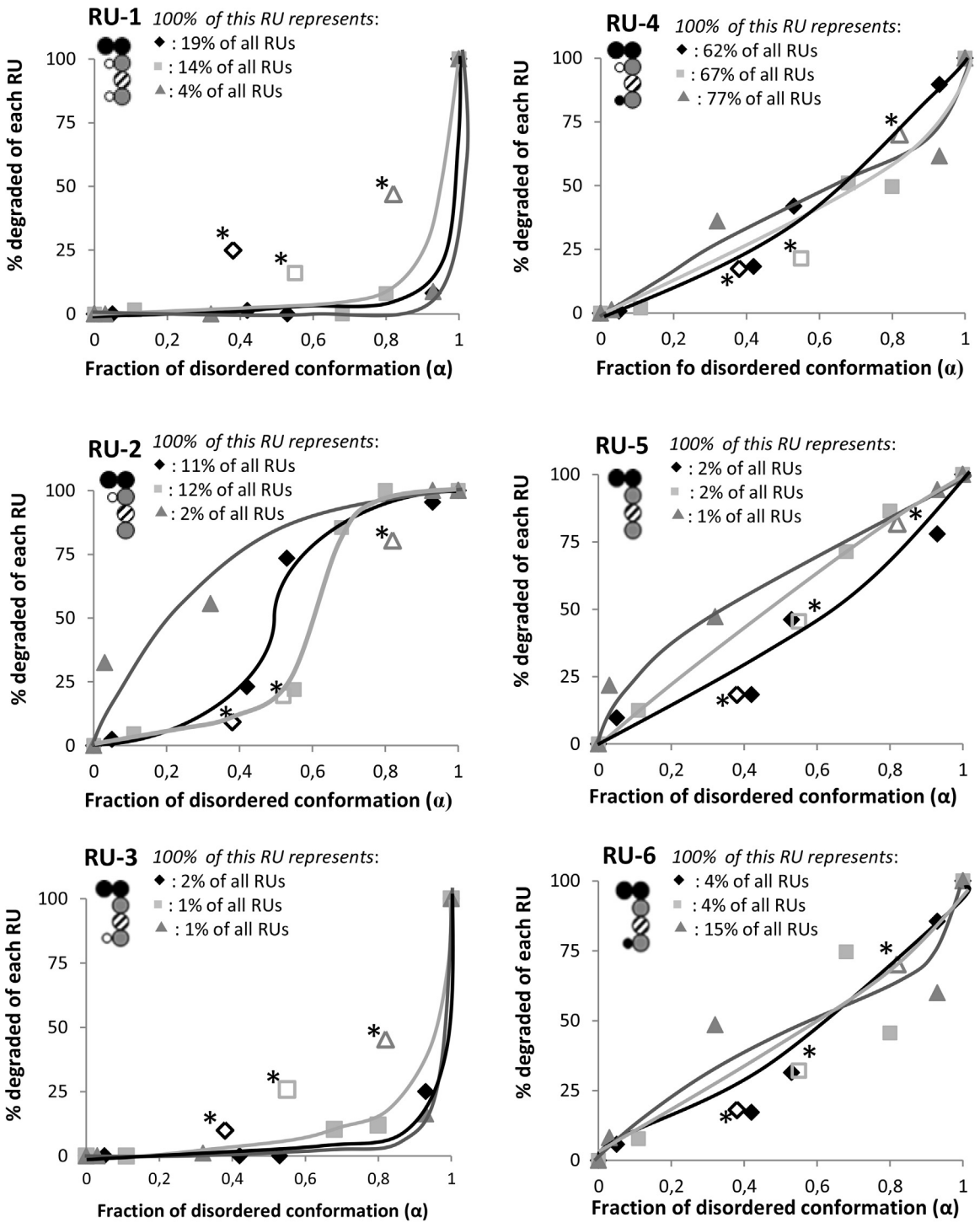

Fig. 4. Degradation pattern of the each xanthan repeating unit, expressed as % of the maximum release of that repeating unit, as function of the xanthan conformation based on HILIC ELSD peak area. Different lines represent the degradation pattern of the RUs in: Xanthan A (♦); xanthan B (■) and xanthan C (▲). Glucose (●); mannose (◍); glucuronic acid (⊘); acetyl group (○); pyruvic acid acetal (●).

of the differences observed in the substitution patterns of xanthan A and B. As xanthan A has a higher acetyl:pyruvate-ratio on the outer mannose than xanthan B (Table 1), it is hypothesized that acetylation of the outer mannose increases the stability of the helical conformation.

The normalized fitted data (not shown) were further used to determine which incubation conditions should be chosen to ensure a specific fraction of disordered conformation. An overview of all incubation conditions and the corresponding xanthan conformations is given in Table 2.

3.2. Molecular weight distribution of xanthan degradation

For the present study it is assumed that, when xanthan appears in a partly disordered conformation, cellulases will completely degrade the disordered parts to the xanthan repeating units (RUs). Furthermore, it is assumed that the enzyme-resistant material consists of ordered xanthan molecules or strongly aggregated xanthan segments as reported previously (Kool, Schols, et al., 2013). This non-degraded material will be detected as high molecular weight material in the HPSEC elution profiles (Kool, Schols, et al., 2013). To determine whether these assumptions indeed apply to the 3 xanthans used in this study, all xanthan digests were analyzed for the molecular weight distribution of the degradation products present. No intermediate degradation products were observed in the elution profiles obtained (data not shown) confirming the assumption made: disordered parts are completely degraded to RUs and enzyme-resistant material, either ordered or aggregated segments remain as high molecular weight material. As a previous study showed that no changes in molecular weight distribution were observed between a 24 h and 48 h xanthan digest (Kool, Schols, et al., 2013), it is assumed that the enzymatic degradation did not result in a conformational change of the non-degraded material to a more disordered conformation. The low molecular weight fractions of the digests obtained at various α can thus be used to study the influence of different primary xanthan structures on the dissociation behavior of xanthan.

3.3. Influence of the constituent repeating units on the xanthan conformation

As only non-aggregated, disordered xanthan segments are susceptible to enzymatic backbone degradation, degradation products present in a xanthan digest must have been part of a disordered xanthan segment. Analysis of the degradation products in xanthan digests obtained at given α will, therefore, enable the correlation between the transitional behavior of xanthan and its primary structure on RU level instead of molar level.

3.3.1. Contribution of the differently substituted repeating units to the stability of the xanthan conformation

Fig. 3 shows the appearance of the individual RUs from 3 different xanthans obtained at various levels of disordered conformation and the dependence of their abundance on the type of xanthan. Clear differences in relative abundance of the RUs at different conformations could be recognized for the 3 xanthans. To enable the correlation between the xanthan conformation and the primary xanthan structure, the presence of each individual RU in the xanthan digests obtained at $\alpha \leq 0.95$ was expressed as percentage of the total amount of that RU present in xanthan (Fig. 4).

Looking at the curves in Fig. 4 three different types of trends can be distinguished for the correlation between the xanthan conformation and the enzymatic release of a RU. An exponential trend is observed for the enzymatic release of the double acetylated RU (RU-1; $R^2 = 0.88$) and the RU which is solely acetylated on the outer mannose (RU-3; $R^2 = 0.89$) when $\alpha \geq 0.8$. The enzymatic release of these RUs thereby follows an exponential trend. Digests obtained after incubation at 60 °C are an exception to this trend, which will be discussed later on. The enzymatic release of the RU that is solely acetylated on the inner mannose (RU-2), follows a Sigmoidal trend ($R^2 = 0.997$). The xanthan conformation range in which this trend is observed differs with the type of xanthan: xanthan A $0.3 \leq \alpha \leq 0.6$; xanthan B $0.5 \leq \alpha \leq 0.65$ and xanthan C $0.0 \leq \alpha \leq 0.4$. Almost maximal enzymatic release RU-2 is obtained already at $\alpha = 0.7$ for all 3 xanthans. The remaining three RUs show a rather linear correlation ($R^2 = 0.957$) between the xanthan conformation and their enzymatic release throughout the range $\alpha = 0$–1. Because pyruvylated RUs, with (RU-4) and without (RU-6) acetylation at the inner mannose, show the same linear correlation between the xanthan conformation and their enzymatic release, the results indicate that acetylation on the inner mannose does not have a significant impact on xanthan's transitional behavior. Segments rich in acetyl groups on the outer mannose (RU-1 and RU-3), however, have a strong stabilizing effect on the ordered xanthan conformation as they are not present in chain segments unfolding easily. Previous studies (Pelletier et al., 2001; Tako & Nakamura, 1984), that assumed that only the inner mannose can be acetylated, concluded that acetyl groups on the inner mannose are responsible for xanthan's conformation stabilization. We now propose that the acetyl groups at the outer mannose strongly contribute to the stabilizing effect of acetyl groups on the xanthan conformation. The substitutions at the outer mannose could, therefore, be key in the xanthan conformation and thus in xanthan's physical properties. As the total degree of substitution on the outer mannose is rather constant between xanthan samples, this could indicate that the acetyl:pyruvate-ratio on the outer mannose determines the transitional behavior of a xanthan sample. As xanthan A contains more RU-1 and RU-3 compared to xanthan B (21% and 15% respectively), these results are in line with the higher transition temperatures observed for xanthan A compared to xanthan B (Fig. 2).

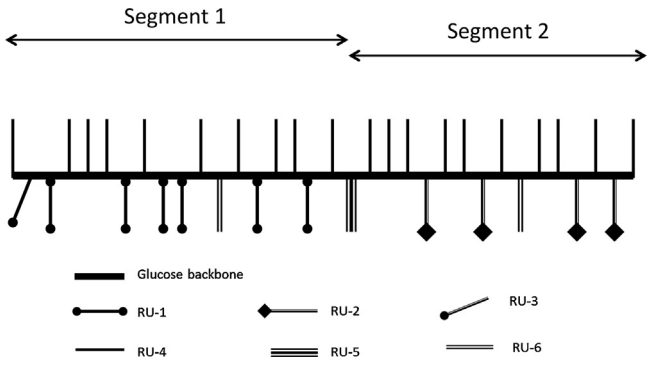

Fig. 5. Hypothetical structure of xanthan as reconstructed from cellulase fingerprinting.

Our results do not necessarily conflict with a previous study reporting that the position of the acetyl groups on either the inner or outer mannose did not influence xanthan's functionality (Hassler & Doherty, 1990). The xanthans used in that study were produced by mutant strains and were either solely acetylated on the inner mannose or solely acetylated on the outer mannose. The disadvantage of the use of such xanthans is that they lack the pyruvate groups. Their solution behavior may, therefore, not be representative for standard xanthan, as used in our study.

Another explanation for the trend observed for the enzymatic release of outer mannose acetylated RUs, is that segments enrich with these RUs are involved in intermolecular interactions. This chain association could results in the formation of aggregated, enzyme-resistant xanthan segments. Dissociation of chains would then be necessary before outer mannose acetylated RUs are susceptible to enzymatic degradation.

3.3.2. Proposed distribution pattern of the xanthan repeating units

The trends observed for the correlation between the enzymatic release of the six types of RU and the xanthan conformation, provides tentative information on the distribution of the different RUs over the xanthan backbone. Assuming that xanthan gradually dissociates to a disordered conformation as described by others (Liu & Norisuye, 1988b; Norton, Goodall, Frangou, Morris, & Rees, 1984),

Table 3
Influence of the solvent conditions on the relative abundance of the repeating units released during the enzymatic xanthan degradation at fixed xanthan conformations.

Incubation condition	Conformation (α)	Total degradation (%)	RU-1	RU-2	RU-3	RU-4	RU-5	RU-6
10 mM NaCl; 60°C	0.48	34	16	16	2	59	3	4
Millipore; 40°C	0.52	37	0	18	0	71	5	6
2 mM NaCl; 55°C	0.78	87	6	25	3	56	5	5
Millipore; 45°C	0.81	85	0	22	0	70	3	5

● glucose; ● mannose; ⊘ glucuronic acid; ○ acetyl groups; ● pyruvic acid ketal

a xanthan molecule can be divided in segments which are either present in an ordered or disordered conformation. If all six RUs are divided over a xanthan molecule in a regular manner, all RUs would be represented in a fixed ratio in all segments which gradually dissociate to a disordered conformation. This would result in a simultaneous and gradual release of each RU by cellulases. As only RU 4–6 follow a linear trend for the correlation between the xanthan conformation and their enzymatic release, a regular distribution of the six RUs over a xanthan molecule cannot explain all trends observed. A different trend would be observed when all RUs would be blockwise distributed and thus be present within distinct segments of the molecule. Each type of RU would then suddenly be released when that specific segment became disordered at a certain fraction of disordered conformation. Such a sudden release at a certain fraction of disorder conformation is only observed for RU 1–3. Both, a regular distribution as well as a completely blockwise distribution can thus not explain all trends observed in Fig. 4.

Fig. 5 shows a hypothetical structure of xanthan as reconstructed from cellulase fingerprinting. Based on the release of the RUs over the fraction of disordered conformation (Fig. 4), a xanthan molecule is divided into segments which are either enriched with RU-1 and RU-3 or with RU-2. Dissociation of these specific segments at a certain disordered conformation explains the sudden release of RUs 1–3. Segments enriched in RU-1 and RU-3 only unfold when $\alpha \geq 0.8$ and segments enriched in RU-2 all unfold at $\alpha \leq 0.6$. A regular distribution of RUs 4–6 over all segments, and thus over the entire xanthan molecule, explains the linear trends observed for the enzymatic release of these RUs as function of the xanthan conformation.

A more precise description of the distribution of the different RUs cannot be given on the basis of the current research. Further research on larger xanthan oligosaccharides, consisting of several RUs, should reveal the exact distribution of the different RUs along the xanthan backbone.

3.4. Interactions stabilisating the xanthan conformation – effect of the solvent conditions on the release of individual repeating units

It is known that different types of molecular interactions are differently influenced by ionic strength and/or temperature: an increase in ionic strength especially reduces the electrostatic repulsion forces through shielding of the negative charges; an increase in temperature reduces electrostatic interactions and reduces hydrogen bonding up to a certain temperature (Creighton, 1993; Damodaran, Parkin, & Fennema, 2008). By studying the influence of the solvent conditions on the unfolding behavior of different xanthan segments it is, therefore, possible to determine which interactions are involved in the stabilization of the xanthan conformation. Xanthan A was used for this. Based on the transition profiles (Fig. 2a), solution conditions were chosen in which the xanthan A conformation was constant (at $\alpha \sim 0.50$ and ~ 0.80), but in which the ionic strength and temperature of the xanthan solutions differed. The relative abundance of the RUs present in the cellulase digests obtained after incubation at the chosen conditions was compared. The results are shown in Table 3. The two digests obtained at elevated temperature (2 mM NaCl 55 °C; 10 mM NaCl 60 °C) were relatively rich in RUs carrying an acetyl group on the outer mannose. The digests obtained at low temperatures in demineralized water did not contain such RUs, but were relatively rich in pyruvylated RUs. Due to the absence of salts in these digests, the negative charges of the pyruvate groups are not shielded. The relatively high abundance of pyruvylated RUs in these digests can thus be explained by increased electrostatic repulsion, making these RUs available for cellulase degradation. As segments rich in outer mannose acetylated RUs only unfolded at elevated solution temperatures, these type of RUs most likely stabilize the xanthan conformation through the formation of hydrogen bonds. Changes in temperature did not influence the dissociation behavior of segments that are rich in RUs that are solely acetylated on the inner mannose. We would, therefore, suggest that especially the acetyl groups on the outer mannose units, and not on the inner mannose, are involved in intra- and/or intermolecular interactions through hydrogen bonding.

4. Conclusions

This study has shown, in contrast to previous reports, that especially those RUs that are acetylated on the outer mannose unit are involved in the stabilization of the ordered xanthan conformation by hydrogen bonding. Acetylation of the inner mannose does not have a significant effect on the conformation stability. Based on the correlation between the α and the enzymatic release of individual RUs it is postulated that pyruvylated RUs are irregularly distributed over the entire xanthan backbone and that double and single acetylated RUs are irregularly distributed within specific xanthan segments. Furthermore, the results suggest that it is possible to control and direct the *exact* transitional behavior of a xanthan molecule by controlling the solvent conditions.

Acknowledgement

Support of this research by the European Community within the consortium PolyModE KBBE-2007-3-3-07 is gratefully acknowledged.

References

Cadmus, M. C., Rogovin, S. P., Burton, K. A., Pittsley, J. E., Knutson, C. A., & Jeanes, A. (1976). Colonial variation in *Xanthomonas campestris* NRRL B-1459 and characterization of the polysaccharide from a variant strain. *Canadian Journal of Microbiology*, *22*(7), 942–948.

Creighton, T. E. (1993). *Proteins: Structures and molecular properties*. New York, NY, USA: W.H. Freeman and Company.

Damodaran, S., Parkin, K. L., & Fennema, O. R. (2008). *Fennema's food chemistry*. Boca Raton, FL, USA: CRC Press, Taylor and Francis Group.

Greenfield, N. J. (2006). Using circular dichroism collected as a function of temperature to determine the thermodynamics of protein unfolding and binding interactions. *Nature Protocols*, *1*(6), 2527–2535.

Hassler, R. A., & Doherty, D. H. (1990). Genetic engineering of polysaccharide structure: Production of variants of xanthan gum in *Xanthomonas campestris*. *Biotechnology Progress*, *6*(3), 182–187.

Jansson, P. E., Kenne, L., & Lindberg, B. (1975). Structure of extracellular polysaccharide from *Xanthomonas campestris*. *Carbohydrate Research*, *45*(12), 275–282.

Jeanes, A., Pittsley, J. E., & Senti, F. R. (1961). Polysaccharide B-1459: A new hydrocolloid polyelectrolyte produced from glucose by bacterial fermentation. *Journal of Applied Polymer Science V*, (17), 519–526.

Kool, M. M., Gruppen, H., Sworn, G., & Schols, H. A. (2013). Comparison of xanthans by the relative abundance of its six constituent repeating units. *Carbohydrate Polymers*, *98*(1), 914–921.

Kool, M. M., Schols, H. A., Delahaije, R. J. B. M., Sworn, G., Wierenga, P. A., & Gruppen, H. (2013). The influence of the primary and secondary xanthan structure on the enzymatic hydrolysis of the xanthan backbone. *Carbohydrate Polymers*, *97*(2), 368–375.

Liu, W., & Norisuye, T. (1988a). Order–disorder conformation change of xanthan in 0.01 M aqueous sodium-chloride – Dimensional behaviour. *Biopolymers*, *27*(10), 1641–1654.

Liu, W., & Norisuye, T. (1988b). Thermally induced conformation change of xanthan – Interpretation of viscosity behaviour in 0.01 M aqueous sodium-chloride. *International Journal of Biological Macromolecules*, *10*(1), 44–50.

Matsuda, Y., Biyajima, Y., & Sato, T. (2009). Thermal denaturation, renaturation, and aggregation of a double-helical polysaccharide xanthan in aqueous solution. *Polymer Journal*, *41*(7), 526–532.

Morris, E. R. (1977). Molecular origin of xanthan solution properties. In P. A. Sandford, & A. Laskin (Eds.), *Extracellular microbioal polysaccharides* (pp. 81–89). Washington, DC, USA: American Chemical Society.

Morrison, N. A., Clark, R., Talashek, T., & Yuan, C. R. (2004). New forms of xanthan gum with enhanced properties. In P. A. Williams, & G. O. Phillips (Eds.), *Gums and stabilisers for food industry* (Vol. 12) (pp. 124–130). Cambridge, UK: The Royal Society of Chemistry.

Norton, I. T., Goodall, D. M., Frangou, S. A., Morris, E. R., & Rees, D. A. (1984). Mechanism and dynamics of conformational ordering in xanthan polysaccharide. *Journal of Molecular Biology*, *175*(3), 371–394.

Orentas, D. G., Sloneker, J. H., & Jeanes, A. (1963). Pyruvic acid content and constituent sugar of exocellular polysaccharides from different species of the genus *Xanthomonas*. *Canadian Journal of Microbiology*, *9*(3), 427–430.

Pelletier, E., Viebke, C., Meadows, J., & Williams, P. A. (2001). A rheological study of the order–disorder conformational transition of xanthan gum. *Biopolymers*, *59*(5), 339–346.

Rinaudo, M. (2004). Role of substituents on the properties of some polysaccharides. *Biomacromolecules*, *5*(4), 1155–1165.

Sandford, P. A., Pittsley, J. E., Knutson, C. A., Cadmus, M. C., Watson, P. R., & Jeanes, A. (1977). Variation in *Xanthomonas campestris* NRRL B-1459: Characterisation of xanthan samples of different pyruvic acid content. In P. A. Sandford, & A. Laskin (Eds.), *Extracellular microbial polysaccharides* (pp. 192–210). Washington, DC, USA: American Chemical Society.

Shatwell, K. P., Sutherland, I. W., Dea, I. C. M., & Ross-Murphy, S. B. (1990). The influence of acetyl and pyruvate substituents on the helix–coil transition behaviour of xanthan. *Carbohydrate Research*, *206*(1), 87–103.

Sworn, G. (2009). *Xanthan gum. Food stabilisers, thickeners and gelling agents*. Oxford, UK: Wiley-Blackwell Publishing.

Tako, M., & Nakamura, S. (1984). Rheology properties of deacetylated xanthan in aqueous-media. *Agricultural and Biological Chemistry*, *48*(12), 2987–2993.